

Psychrometric Wet Elements as a Basis For Precise Physico-Chemical Measurements*

Russell G. Wylie

National Measurement Laboratory, Sydney, Australia 2070

October 30, 1978

Under appropriate conditions, psychrometric wet elements of simple design can be highly reproducible in behavior. A temperature depression of 10 K can be reproducible from element to element within 2 mK. The properties of a wet element can be determined very accurately by direct comparisons with other wet elements in a common airstream. Comparisons with one specially developed type show the effects of practical water-retaining coverings. Comparisons with another type, which simulates the fully calculable flat-plate system, then give the behavior in absolute terms.

A cotton-yarn covering increases the psychrometer coefficient A by only 0.2 percent. The departure of the flow around a cylinder from laminar boundary-layer flow increases it by 0.7 percent.

The background and theory are outlined. The detailed behavior of cotton-yarn covered cylinders is deduced from element comparisons; and their absolute value of A obtained as a function of diameter, airspeed, and the temperature, pressure and water content of the airstream. The dependence of A on these parameters is essentially simple. The work leads to a large increase in the accuracy of water vapor measurements and to new methods of measuring some other physico-chemical quantities.

Key words: Convective heat transfer; convective mass transfer; emissivity of water; evaporation coefficient; humidity measurement; monomolecular film; psychrometer; psychrometry; radiative heat transfer; temperature depression; water vapor measurement; wet bulb; wet element.

1. Introduction

1.1 General Background

The instrument for which August [1825]¹ coined the term "psychrometer" utilizes the steady depression of the temperature of a wet temperature-sensing element to determine the water vapor content of an airstream. It originated in devices employed by Hutton [1792], Leslie [1799], and Böckmann [1803]. The last-named and possibly earlier workers understood that the wet-element temperature depended not only on the temperature and vapor content of the air, but also on the airspeed. Belli [1830] reported that it further depended on the size and shape of the wet element, but that the effects of changes in the airspeed and in the size and shape of the element were greatly reduced when the airspeed was raised to a few metres per second.

When Belli recommended that an adequate airflow should be provided, all the essential features of the ventilated psychrometer as widely used today had been established. Nevertheless, the literature on psychrometry has grown to more than 1000 references, concerned mainly with a great variety of designs involving practically every conceivable

method of measuring temperature, formulas for deriving the air water content, the theory, sources of error, work with gases and liquids other than air and water, and special applications. However, progress on fundamental aspects has been slow.

The subject has been reviewed at length by Sonntag [1967] who has cited 850 references. Sonntag has, however, missed some important contributions; for example, Sherwood [1937], Bedingfield and Drew [1950], Fuchs [1959], and Dahlen [1962]. The selective account by Bongards [1926] and the selective bibliography by Sinha [1963] with a foreword by Rigby are still of value.

The steady temperature of a properly designed psychrometric wet element is such that there is a balance between the heat influx of the convective and radiative heat-transfer processes and the heat efflux of the evaporation process. We will assume as a boundary condition that the surface temperature of the wet element is uniform. Theoretically, it is shown below that the surface temperature is inherently almost uniform, and experimentally, it is shown that for the elements used in the present work, which conduct heat very well internally, the effect of the residual nonuniformity is negligible.

A surface-average heat-transfer coefficient h for the combined convective and radiative heat fluxes may be defined

* Invited paper.

¹ Dates in brackets indicate literature references at the end of this paper.

with respect to $T - T_o$, where T is the temperature of the stream and T_o that of the wet surface. Similarly, a surface-average mass-transfer coefficient k for the vapor flux may be defined with respect to $x_o - x$, where x is the vapor mole fraction in the stream and x_o the saturation mole fraction for the temperature T_o . Upon equating the enthalpy fluxes, the usual psychrometer equation

$$(x_o - x) = A(T - T_o) \quad (1)$$

is obtained, with the psychrometer coefficient A given by

$$A = h/(kL), \quad (2)$$

where L is the heat of evaporation for the conditions at the surface. When h is regarded as defined for the finite temperature difference $T - T_o$ and in the presence of the mass-diffusion process, and k as being analogously defined, the equations are exact.

A change in the value of A of, perhaps, 10 percent, corresponds to a surprisingly small increment in humidity. For example, for 20 °C and a relative humidity of 50 percent, a reduction of this amount in A changes the derived relative humidity only to 51.7 percent. Conversely, in a direct experimental determination of A , the result is sensitive to a knowledge of the conditions. The values in general use, notably the values obtained by Ferrel [1885] for a whirling psychrometer and those given by Sprung [1888] for the Assmann psychrometer [1887], have been determined experimentally for particular instruments. They approximate $6.7 \times 10^{-4} K^{-1}$.

Of two major inconsistencies that remain in the literature, one concerns the effect of the ratio of the diffusivity of the vapor to the diffusivity of heat. The theory of the wet element has been developed on sound lines since 1932, as considered below. A number of experimenters have since obtained results by using a series of organic liquids as well as water in order to involve a range of the diffusivity ratio. As a rather profound simplification occurs in the theory when this ratio is unity, values differing considerably from unity are necessary for a proper comparison. For water in air the ratio is 1.19; but with organic liquids, values of 4 or more are feasible.

Bedingfield and Drew [1950] have re-analyzed the best of those results and contributed some of their own results for volatile organic solids. The correlated results imply that the Prandtl number enters the heat-transfer coefficient as the factor $Pr^{0.44}$ (and equally, the Schmidt number enters the mass-transfer coefficient as the factor $Sc^{0.44}$). However, many experiments, including those with liquid drops reviewed by Fuchs [1959] and the careful experiments of Dahlen [1962] with unusually smooth wet cylinders, point to an index closer to one-third. Boundary-layer theory, as referred to below, and the results given by Zukauskas [1972] indicate that for a cylinder in a transverse stream, the index is close to 0.37.

On the basis of this value, the conclusions of Bedingfield and Drew mean that as the diffusivity ratio increases from unity to 4, the experimental value of the psychrometer coefficient declines relative to the theoretical value by 10 percent.

The second major inconsistency, which has existed for more than 40 years, is that accepted experimental values of the psychrometer coefficient for water in air are about 8 percent greater than theoretical values. The present work, which is concerned solely with water in air, resolves this discrepancy with the finding that the experimental values are too high.

1.2 Outline of the Present Work

In the present paper the theory is outlined, and the theoretical properties of the psychrometer coefficient are summarized. Some very accurate experiments are then described which build up a knowledge of the properties of three types of wet elements. The observed properties are accurately consistent with the theory when very small, constant adjustments are made to the psychrometer coefficient for an effect of cotton water-retaining coverings and an effect of the departure of the flow around a cylinder from laminar boundary-layer flow. The work leads to a very substantial increase in the accuracy of psychrometric water vapor measurements, and to new methods of measuring some other physicochemical quantities that are difficult to measure otherwise.

A high reproducibility of the behavior of the wet elements, not only for a given element but from element to element of a given type, has been achieved by some special but simple features of their design and use. The special features of their design are a thermally highly conducting core; a water-retaining covering, which makes a uniform and close thermal contact with the core; and thermal guards. The special features in their use are a well-defined environment as regards radiative heat transfer, and the routine removal of residual organic films from their wet surfaces.

The types of elements are cotton-yarn covered cylinders, cylinders with thin grooved stainless-steel coverings, and cotton-yarn covered blades with a cross section approximating a narrow-angled wedge. The cotton-yarn coverings are helical or quasi-helical windings. The stainless-steel surfaces have sharp-crested helical grooves in which water is supported by surface tension.

The high accuracy of the experiments is attributable to the reproducibility of the elements and a method of determining the difference between the psychrometer coefficients of two elements by mounting them in a common airstream and measuring their temperature difference—a fully developed version of a method introduced much earlier by the author [1949]. Repeated comparisons of the same two elements show the accuracy of the comparison technique and the reproducibility of the behavior of a given element, while

comparisons of different elements of a given type show the reproducibility from element to element. Comparisons of elements which differ appropriately show the effects of differences in type or size or other features.

The cotton-yarn covered cylinders are simply convenient practical elements which satisfy the design criteria and may be used for most applications of the work. The other two types of elements have been developed to have special properties so that specific information is gained about elements compared with them. The cylinders with grooved stainless-steel coverings are shown below to be accurate simulators of smooth cylinders of water. Cylinders with other water-retaining coverings may be compared with them to determine the effect of the coverings. The cotton-yarn covered blades are shown to be accurate simulators of the classical flat-plate system, allowance being made for the effect of the covering. The absolute value of the psychrometer coefficient for these elements can, therefore, be calculated by using the theory outlined; and the value for any other type of element can be obtained from comparisons with them.

Element-comparison results given below show that a cotton-yarn covering increases the psychrometer coefficient by only 0.2 percent and that the departure of the flow around a cylinder from laminar boundary-layer flow increases it by only 0.7 percent. They also yield the absolute value of the psychrometer coefficient for a cotton-yarn covered cylinder (as well as those for the other two types of elements) with an uncertainty of about 1 percent attributable almost entirely to the uncertainties in the data available for the thermal conductivity of air and the diffusivity of water vapor in air.

When the results of the theory and the experiments are considered together, it becomes clear that A can be deduced with an uncertainty of about 1 percent for elements of a variety of types and a range of sizes and airspeeds. It can then be seen that the values at present in general use have a positive bias of several percent. The work shows that psychrometric water vapor measurements can be made with the high absolute accuracy that corresponds to an uncertainty of 1 percent in A , or 0.3 percent having regard to direct measurements of A to be published by Wylie and Lalas, and differential water vapor measurements with the high relative accuracy that corresponds to 0.05 percent in A . Further, the work has already led to new methods of measuring the evaporation coefficient of water, the evaporation resistance of a monomolecular film on water for very low levels of resistance, and convective heat-transfer coefficients for wet surfaces.

2. Theory

The author has made a detailed theoretical analysis for laminar boundary-layer flow, based on complete equations for heat and vapor diffusion in a moving gas (Bird, Curtiss and Hirschfelder [1955]). This will be published. In the

following outline, the secondary effects can only be introduced rather arbitrarily. The problem is to calculate the quotient h/k in eq (2) for particular wet elements as a function of the airspeed, and of the temperature, pressure and water content of the airstream.

2.1. The Radiation and α Effects

First, we separate out the effects of the radiative heat transfer and the molecular-kinetic resistance to evaporation localized at the liquid surface and associated with the evaporation (equally condensation) coefficient α . We will term the latter the α -resistance. The convective and radiative heat fluxes are simply additive. Associating them with heat-transfer coefficients h_c and h_r we have

$$h = h_c + h_r = h_c \left(1 + \frac{h_r}{h_c} \right). \quad (3)$$

If the vapor mole fraction adjacent to the liquid surface is x'_0 , the convective resistance to evaporation is associated with $x'_0 - x$ and the α -resistance with a small discontinuity $x_0 - x'_0$ at the surface. These resistances are in series, and so in terms of the corresponding mass-transfer coefficients k_c and k_α , which are in the nature of conductances, we have

$$k = \frac{k_c k_\alpha}{(k_c + k_\alpha)} = \frac{k_c}{\left(1 + \frac{k_c}{k_\alpha} \right)}. \quad (4)$$

Putting eqs (3) and (4) in eq (2) we have

$$A = A_c \left(1 + \frac{h_r}{h_c} \right) \left(1 + \frac{k_c}{k_\alpha} \right), \quad (5)$$

where

$$A_c = h_c / (k_c L). \quad (6)$$

We will call A_c the convective psychrometer coefficient. Like h_r , k_α is not only the surface-average coefficient, but also the uniform local coefficient; but the local k_c is not uniform. Therefore eq (4), in which k and k_c are surface averages, is an approximation. However, the accuracy with which k_α is known is seen below to be relatively low; and numerical studies have shown that the equation is adequate for present purposes.

The bracketed factors in eq (5), respectively, the radiation and α factors, must be evaluated as a separate issue, by using data obtained experimentally. The α factor has not appeared in earlier work. In these factors, h_c and k_c do not need to be of the high accuracy sought for h_c/k_c in eq (6); and a coefficient k_c may be used which is obtained from h_c as in Appendix B. Formulas for the transfer coefficients which provide for present purposes are given in that appendix.

Choosing approximately the extremes in the present experiments, the radiation and α factors for a 5 mm cylindrical element at 10 m/s are 1.037 and 1.015, respectively, and for a 10 mm element at 1 m/s are 1.168 and 1.003, respectively.

2.2. Main Argument

The problem has become the calculation of h_c/k_c in eq (6).

Neglecting for the moment the effects of the net efflux of gas from the surface, the interactions of the heat- and vapor-transfer regimes and the variation of the properties of the gas mixture with temperature in the range T_o to T and vapor mole fraction in the range x to x_o , we note that the appropriate approach is that first indicated by Colburn [1932] and followed by Sherwood [1937]. In effect this recognizes that, with the present boundary conditions and the neglect of the effects mentioned, the heat- and mass-diffusion processes in the moving gas are mathematically similar. In terms of the usual dimensionless groups (defined in appendix B), Sh is then the same function of Re and Sc as Nu is of Re and Pr . For laminar boundary-layer flows, theory shows that this function is at least closely approximated by a product of a function of Re and a function of Pr or Sc (Schlichting [1968]; Bird, Stewart and Lightfoot [1960]). That is, for the convective heat transfer.

$$Nu = bf(Re)\phi(Pr), \quad (7)$$

while for the convective mass transfer

$$Sh = bf(Re)\phi(Sc), \quad (8)$$

where the constant b and the functions f and ϕ are the same in both, and $\phi = 1$ when $Pr = 1$.

Dividing eq (7) by eq (8) we have

$$\frac{h_c}{k_c^o} = \left(\frac{\lambda}{cD}\right) \frac{\phi(Pr)}{\phi(Sc)}, \quad (9)$$

where λ , D and c are, respectively, the thermal conductivity, the vapor diffusivity, and the total mole density of the gas; and where the superscript in k_c^o recognizes the neglect thus far of the net flow of gas from the surface. This flow has with some reason been called by Fuchs [1959] and others the Stefan flow.

The principal effect of the Stefan flow is that the vapor flux at the surface is not simply the product of the diffusivity and the gradient of x ; but involves a further factor $(1 - x_o)^{-1}$, as may be seen in Bird, Stewart, and Lightfoot [1960]. That is, $k_c = k_c^o/(1 - x_o)$. Thus, on combining eqs (6) and (9) we obtain

$$A_c = (1 - x_o) \left(\frac{\lambda}{cDL}\right) \frac{\phi(Pr)}{\phi(Sc)}. \quad (10)$$

A number of authors have since presented substantially this same treatment, but some have missed the factor $(1 - x_o)$. Kusuda [1965] has given a closely related treatment for the flat plate, focusing attention on a Lewis number rather than A , and substituting carefully selected data. Because of inappropriately defined mass-transfer coefficients, partly carried over from Eckert and Drake [1959] and Threlkeld [1962], he too has missed the factor $(1 - x_o)$, although he has included the smaller effect of the Stefan flow described below. Because he has used the mixing ratio as a mass-transfer potential, his formation is otherwise valid only when x is small or near the saturation value.

On the usual basis of the Prandtl boundary-layer equations (Schlichting [1968]), $\phi(Pr)$ can be calculated for the flat plate by numerical methods, and an accurate formula obtained by the author is given in Appendix B. For that system and the present values of Pr and Sc , ϕ approximates $Pr^{0.36}$, and for the other extreme of a leading stagnation line $Pr^{0.37}$, as implied by the calculations of Squire [1938] and Makarevičius and Zukauskas [1972]. For a whole cylinder, Zukauskas [1972] finds again an index of 0.37. As Pr and Sc for water in air are not very different, approximating 0.72 and 0.61, respectively, A_c is not particularly sensitive to the form of ϕ . The change in $\phi(Pr)/\phi(Sc)$ for a change of 0.01 in the index is only 0.17 percent.

To obtain x_o , the saturation pressure of pure water vapor divided by the prevailing pressure must be multiplied by the factor f_w defined by Goff [1949]. Calculated from recent data (see Appendix B), f_w for water in air at atmospheric pressure is found to be 1.0041 for T_o from 0 to 20 °C. Also, L is slightly less than for pure water. A formula for atmospheric pressure is given in Appendix B. For the T_o of the present experiments the reduction is 8 in 10^4 .

2.3. The Secondary Effects

These are small, and each may be calculated as a separate perturbation of the regime already considered. In the following, the percentages in brackets are, respectively, the largest component effect and the whole effect of the particular mechanism on h_c/k_c and hence A_c for the present experimental conditions.

As well as contributing the factor $(1 - x_o)$ in eq (10), the Stefan flow affects the velocity boundary condition at the surface and hence the velocity field, affecting h_c and k_c in analogous ways. Various approximate treatments of the effects for heat and mass transfer have been given by Bird, Stewart, and Lightfoot [1960] who have also made an application to the psychrometer; but the rather general results obtained by Stewart [1963] are particularly appropriate for psychrometer theory (-0.25% ; -0.02%). A small effect which arises from the fact that the field equation for the temperature is most closely related to the mass average velocity, while that for the vapor mole fraction is most closely

related to the mole average velocity, has been partly considered by Bedingfield and Drew [1950]. The author has considered all the differences in form of the largely similar equations (-0.09% ; -0.04%).

The effects of the variations of the fluid properties (λ , c , D , the dynamic viscosity μ and the mass density ρ) with T and x in the boundary layer have been obtained theoretically by the author [1973]. Provided the dimensionless groups in eqs (7) and (8), and hence all the quantities in eq (10), are evaluated for the surface temperature T_o and mole fraction x_o , then for water in air the effect on h_c due to λ and μ practically cancels with that of c and ρ . Because of gas-kinetic relationships and the near equality of Pr and Sc , a similar situation occurs for k_c and, furthermore, the residual effects on h_c and k_c practically cancel ($+0.20\%$; $+0.03\%$).

Finally there are the diffusion-thermo and thermo-diffusion effects which, unlike the aforementioned, are not of the second order and so do not vanish as $T - T_o$ and hence $x_o - x$ approaches zero. They can only be obtained approximately, because the thermal diffusion factor for water in air, calculated by Mason and Monchick [1965], is uncertain within a factor of about two. The author has estimated them by defining effective values of λ and D for substitution in eq (10), including the dimensionless groups (-0.07% ; -0.02%).

The aggregate of these effects, which are uniform over the surface, is a decrease of only 0.05 percent. It is insensitive to the temperature, pressure and water content of the airstream; and we will here regard it as a constant correction to eq (10).

Now, hardly a word of the text of section 2.2 up to eq (10) would need to be changed if the alternative were adopted of defining h_c and k_c to be the conventional local values, which relate, respectively, to the heat and vapor fluxes at a point on the surface. Corresponding local Nusselt, Sherwood and Reynolds numbers may be defined which, instead of the overall length parameter d introduced in Appendix B, contain a suitably chosen length parameter, say s , which relates to the position of the point on the surface and in simple cases is the distance of the point from the leading stagnation line (or point) measured along the surface. The form of eqs (7) and (8) is still a good approximation. The factor b and the function f are in general changed, but the function ϕ is practically the same as before.

When eq (7) is divided by eq (8) to get eq (9), the s in Nu cancels with that in Sh , and $f(Re)$ cancels out, leaving the quotient h_c/k_c^o , and equally h_c/k_c , independent of s . However, this is simply the condition for the equilibrium surface temperature of the hypothetical purely convective wet element ($h_r = o$ and $k_\alpha \rightarrow \infty$) to be uniform, and so, to the extent that the form of eq (7) is accurate, the temperature boundary condition assumed in section 1.1 is confirmed for such an element. Further, eq (10) shows that, both for the purely convective element and for the practical element

which includes the effects of radiation and the α -resistance, the local value of A_c is practically uniform over the surface.

2.4. Theoretical Properties of the Psychrometer Coefficient

A_c has been found above to be uniform over the surface. Also, in view of eq (10) and the fact that $\phi(Pr)$ is practically the same for different laminar boundary-layer flows, A_c is practically the same for all such flows. Indeed, as equations of the form of eqs (7) and (8) with much the same ϕ as for laminar flows are generally used also for turbulent and separated flows, there is some expectation that the theory is reasonably accurate for these flows as well. In fact it is reasonably accurate for a cylinder in a transverse stream, a system that involves an extensive area of separated boundary layer; for it is shown experimentally below that A_c for that system exceeds the flat-plate value by only 0.7 percent, part of which can be attributed to the index of Pr in ϕ being a little greater for the cylinder than the flat plate.

The actual surface temperature must depart slightly from uniformity because, while in accordance with eqs (7) and (8) the local convective heat- and mass-transfer coefficients vary markedly but in proportion over the surface, h_r and k_α are uniform. Therefore, defined in terms of local convective transfer coefficients, the radiation and α factors in eq (5) vary over the surface. A significant variation of T_o would destroy the similarity of the temperature and mole-fraction boundary conditions, for where the local $T - T_o$ decreased, the local $x_o - x$ would increase. Equations (7) and (8) would be affected in different ways. However, the variation is shown below to have been negligible in the present work.

It is convenient to define B_c in general by writing

$$A_c = (1 - x_o) B_c. \quad (11)$$

Then from eq (10) we have

$$B_c = \left(\frac{\lambda}{cDL}_o \right) \frac{\phi(Pr_o)}{\phi(Sc_o)}, \quad (12)$$

where the subscript indicates evaluation for the conditions at the surface. At constant T_o , B_c is independent of T and, as λ , c , D , L , Pr and Sc have practically no direct pressure dependence, depends only very slightly on the pressure through the small dependences of λ , c , D , Pr and Sc on x_o . Further, it is found that its small dependence on T_o is practically linear. For the flat plate at approximately atmospheric pressure, and T_o of 0 to 60 °C.

$$B_c = 5.79 \times 10^{-4} + 7.0 \times 10^{-7} T_o K^{-1}. \quad (13)$$

The absolute uncertainty in this is about 1 percent which arises almost entirely from the data available for λ and D .

These two quantities occur in Pr and Sc as well as explicitly in eq (12).

Putting eq (13) in eq (11) gives A_c , which is found to have a very shallow maximum with respect to T_o . For atmospheric pressure, this occurs near 16 °C. The nominal T_o in the present experiments (15 °C) is close to this value, and the corresponding A_c for the flat plate with a smooth water surface may be regarded as constant at $5.79 \times 10^{-4} K^{-1}$ (within 0.2% for T_o from 10 to 25 °C). The dependence of A_c on the pressure, which arises almost entirely from the factor $(1 - x_o)$, is slight in the present temperature region but increases rapidly as T_o approaches the boiling point.

3. Experiments

3.1. Experimental Details

The construction of the cores for cylindrical elements with cotton-yarn or grooved stainless-steel coverings is shown in longitudinal section in figure 1(a), and the cross section of the bladelike cores for flat-plate simulators, used only with cotton-yarn coverings, is shown in figure 1(b). In figure 1(a), cotton-yarn coverings extend over the areas A and B. Stainless-steel coverings extend over the area A while the areas B are provided with cotton guards. To allow the rapid removal and replacement of stainless-steel coverings for

cleaning purposes, cores used with them have removable nosepieces. At the rounded tips of cylinders and the plane ends of blades, the coverings are completed with thin paper of pure cellulose. Also, the supporting stems of blades are provided with cotton guard coverings.

Cotton-yarn and stainless-steel coverings on cylinders, with an overall diameter of 10 mm, are seen both dry and water-charged in figure 2. Loose-spun thread of 90 mg/m, forming windings of about 27 turns per cm, has been used. Stainless-steel coverings have sharp crests of 60° included angle, a root to crest height of 0.31mm and a pitch of 0.79 mm. Their inside surfaces are cylindrical and their wall thickness at the root is 0.25 mm. A cotton-yarn winding inherently makes a close and uniform thermal contact with the core. For a stainless-steel covering, such a thermal contact is achieved by allowing a diametral clearance of only 0.05 mm to the core and filling the clearance space with the liquid being used, which is water in the present experiments.

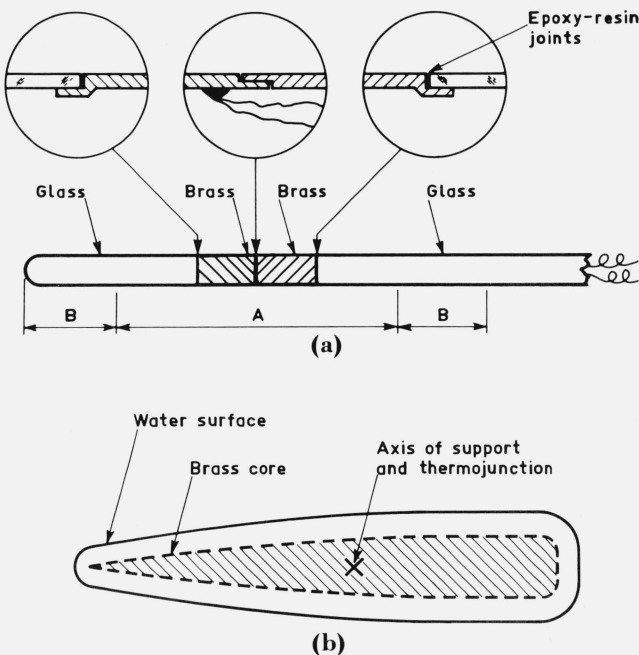


FIGURE 1. (a): Construction of the core of a cylindrical wet element. When a grooved stainless-steel covering is used, it occupies section A while cotton guards occupy sections B. The nose section B is then not quite as shown, being made readily removable. (b): Cross-sectional form of the wedge-like flat-plate simulators.

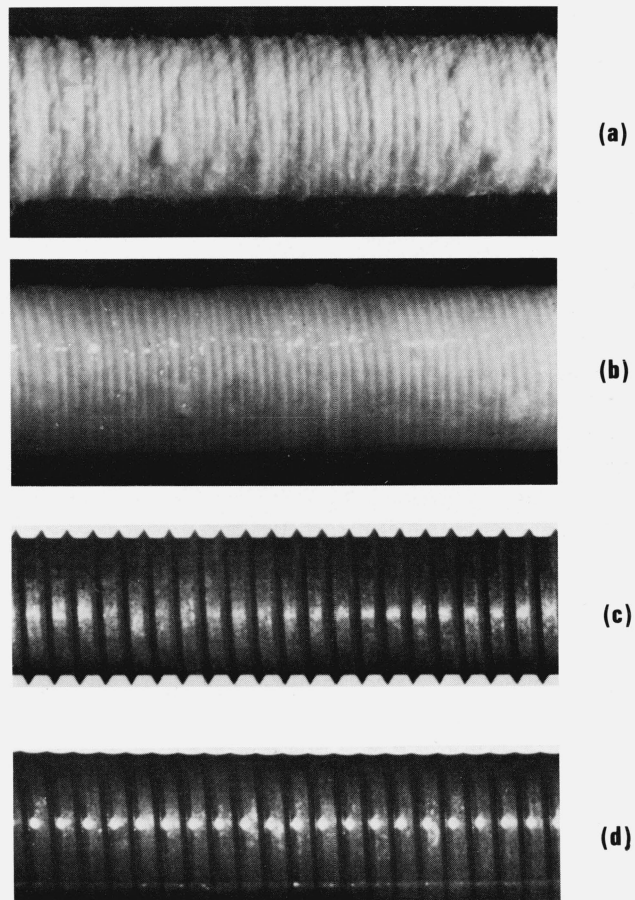


FIGURE 2. Wet-element coverings typical of those used. (a) and (b): A helical winding of cotton yarn, (a) dry and (b) fully wet. (c) and (d): A stainless-steel tube with sharp-crested helical groove, (c) dry and (d) fully charged with water.

Cotton yarn should be degreased, boiled in successive portions of distilled water, and dried, before being wound on a core without contact with the bare hands. The importance of removing any organic films from the subsequently wetted surface is shown below. Stainless-steel coverings are cleaned initially and at frequent intervals by heating to a dull red heat in a silica tube. They must not then be touched with the bare hands.

Element comparisons have been made in the small wind tunnel seen in figure 3. The elements are mounted parallel on a unit which plugs into the tunnel wall and allows them to be rotated to different angular positions while horizontal, at a fixed separation, and perpendicular to the airstream. A standard axis-to-axis separation of three times the diameter of the cylinder, or cylinders, involved has been adopted. A unit fitted with a cotton-yarn covered and a stainless-steel covered element, both of 10 mm overall diameter, is seen in the figure. The units are readily detached from the tunnel for the final removal of organic films, and element inspection and rewetting.

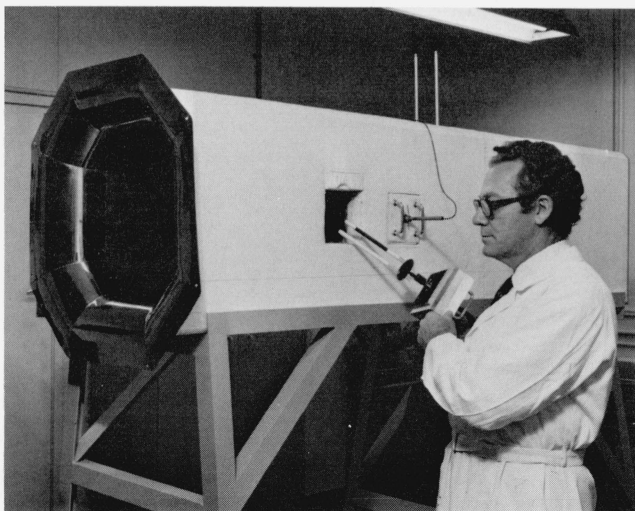


FIGURE 3. General view of the small wind tunnel, showing its bell-mouth and facing radiation shield (left).

A unit comprising a 10 mm cotton-yarn covered wet element and a 10 mm wet element with grooved stainless-steel covering is being inserted.

The inside surface of the tunnel is of wood finished with matt-black enamel, while the bell-mouth is of metal and chromium plated. These surfaces are thermally insulated with polystyrene foam on the outside. A matt-blackened radiation shield of copper, backed with such foam, is suspended opposite the tunnel entrance, as seen in figure 3. This fills the view from the wet elements through the entrance. These features to control the radiation conditions are important, for if the surfaces seen by a 10 mm element in an airstream of 1 m/s under the present experimental

conditions were uniformly raised in temperature by 1 K, the temperature of the element would rise by 56 mK.

A copper-constantan thermocouple of fine wire is used differentially between the elements, the emf being amplified and continuously displayed on a chart recorder. By providing the elements with temporary close-fitting sheaths and immersing them in a small, stirred water bath, a "thermal zero" is obtained which is subtracted from the observations. This has rarely exceeded 2 mK and has usually been repeatable within 0.5 mK after an experiment.

The airspeed is measured with a static tube referenced on the atmosphere outside the tunnel. Used with a sensitive bubble manometer, this gives an airspeed accuracy ranging from about 2 percent at the minimum of 0.5 m/s to better than 1 percent at the maximum of 11 m/s. It is known from precise heat-transfer studies made in the tunnel that the free-stream turbulence intensity is approximately 1 percent. Except at the higher Reynolds numbers, the turbulence has no detectable effect (<1%) on the heat-transfer coefficients and may be expected to have an effect very much smaller than 1 percent on A_c . The maximum Reynolds number or airspeed for this regime corresponds to the kink in the $Nu(Re)$ relationship as given in Appendix B.

The stream temperature is measured with calibrated secondary-reference mercury-in-glass thermometers (B.S.1900:1952) inserted through the top of the tunnel, and the stream water content with a reference psychrometer comprising a 5 mm cotton-yarn covered cylindrical wet element and a parallel dry (uncovered) element mounted transversely in the tunnel. The pressure is measured with a Fortin barometer. The diameters (sizes) of the water-charged wet elements are obtained by comparison with metal rods using a low-powered microscope.

It may be noted that the effective temperature of the air incident on the elements and thermometer bulbs exceeds the true air temperature by a small amount proportional to the square of the airspeed—the adiabatic wall effect discussed by Schlichting [1968]. However, the effect has been found experimentally to be practically the same for a cylinder and a flat-plate simulator (40 mK for 10 m/s); and as it is included in the measured stream temperature, no related adjustments to any of the observations are necessary.

The following experiment shows that monomolecular films are detrimental, but that they can easily be removed. Two cotton-yarn covered cylindrical elements 5.2 mm in diameter were mounted as a two-element unit and operated in the wind tunnel in a vertical plane at an airspeed of 2.55 m/s. The steam temperature and wet-element temperature depression approximated, respectively, 22 °C and 7 degrees. Starting with clean wet elements and removing the unit from the tunnel as required, an oleic acid monolayer was formed on one wet element by passing it through a water surface bearing a proven monomolecular film in equilibrium with a small

excess of the substance. The observed steady temperature difference of the elements in the airstream and the corresponding percentage difference of their values of A are the first entries in columns 1 and 2 of table 1. The film was then removed by flooding the element with pure water from a device like a chemist's washbottle, the film being progressively carried away on the surfaces of the drops falling from the element. The temperature difference then observed and the corresponding percentage difference in A are given in columns 3 and 4. The procedure was then repeated but with the film formed on the second element, giving the results in the second line of the table. The results in successive lines were obtained with films formed alternately on the elements.

TABLE 1. *Effects of addition and removal of oleic acid monolayers*

ΔT_o with a film on one element mK	Equivalent $(\Delta A)/A$ %	ΔT_o with the film removed mK	Equivalent $(\Delta A)/A$ %
-19.5	-0.77	-0.5	-0.02
+21.0	+0.83	+1.0	+0.04
-20.0	-0.79	+0.5	+0.02
+17.5	+0.68	-2.0	-0.08
-23.5	-0.92	+0.5	+0.02
+19.5	+0.77	-0.5	-0.02
-24.0	-0.94	0	0
+19.5	+0.77	+1.0	+0.04

The effect of an oleic acid monolayer on the rate of evaporation of water in air is so small that it generally escapes detection, as instanced by Jarvis, Timmons, and Zisman [1962]; but the present method easily shows the effect, here averaging 21 mK. A similar experiment with films formed from the natural grease of the hands gave an average effect of 290 mK, but as this substance is a complex mixture of compounds it could not easily be proven that the films were monomolecular. They were just as easily removed. It is found that even with careful assembly and wetting, films detectable by the present methods are rather likely to be present initially. However, the flooding procedure easily removes them, and has been applied routinely.

3.2. Effect of Water Depletion

Because it is much more convenient to charge the elements with water at the beginning of each run than feed them continuously, we must know the effect of the subsequent depletion by evaporation. This has been determined by

recording the temperature difference between an element initially charged with water and another element on which the water is maintained at a fixed water tension by a capillary feed. For 5 mm cotton-yarn covered cylinders charged with water at room temperature and inserted in an airstream of 5 m/s which is at 22 °C and gives a temperature depression of 7 degrees, it has been found that the initial transient of about 2.5 min duration is followed by a period of approximately 2.3 min during which the temperature is constant within 2 mK. Observations for various diameters and airspeeds show that the period of constant temperature is inversely proportional to the rate of evaporation, as would be expected.

The results of water-depletion experiments for grooved stainless-steel surfaces have more implications. Figure 4 shows the temperature change of a 5 mm grooved element at 5 m/s, again charged with water at room temperature and inserted in an airstream at 22 °C which gives a temperature depression of 7 degrees. When the initial transient of about 1 min duration has disappeared, the temperature remains constant within 1 mK for 3 min, apart from fluctuations. It then briefly decreases 3 or 4 mK as the liquid becomes tangential at the crests and some thermal radiation which passes through the water near the crests is reflected back from the metal and lost. Finally the temperature rises rapidly as the meniscus retreats from the crests, exposing bare metal. Again, results for different diameters and airspeeds show that the time-scale varies inversely with the rate of evaporation.

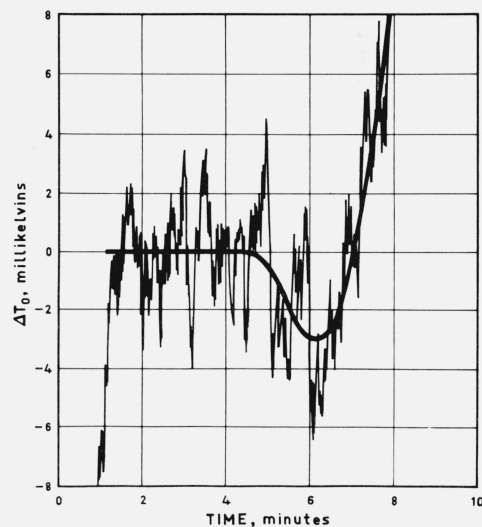


FIGURE 4. *The temperature change (as recorded) of a 5 mm wet element with grooved stainless-steel covering as its water charge is depleted by evaporation in an airstream of 5 m/s.*

Temperature depression 7 K. The temperature is constant within about 1 mK for 3 min, after which a small drop (see text) occurs before a rapid rise due to the onset of dryness at the stainless-steel crests.

Direct measurements of the heat-transfer coefficient for the water-charged stainless-steel surfaces have shown that the coefficient based on the apparent surface area (area of the cylinder of the crest diameter) remains practically constant until the water surface is almost tangential at the crests. Further, the emissivity of water being very high (98%), the radiative heat-transfer coefficient based on that area also remains practically constant. Consequently, the radiation and α factors in eq (5) remain constant during evaporation although the shape of the surface changes substantially, and so the observed constant temperature is consistent with A_c being unaffected by that change. More important for present purposes, as the interval of constant temperature in figure 4 can obviously be extrapolated backwards to a surface fully charged with water, the temperature observed is that of a smooth cylinder of water whose diameter is the crest diameter.

The behavior of the flat-plate simulators is generally similar to that of the cotton-yarn covered cylinders. There is no difficulty in ensuring that the observations adopted in element comparisons have been made within the constant temperature periods of both elements.

3.3. Reduction of the Observations

The observed temperature difference relates to elements which depart slightly in size from the nominal and experience local airspeeds which are slightly different from the free-stream value because of a slight hydrodynamical coupling between the elements. Each element intercepts some of the thermal radiation from the other and is exposed to a stream differing slightly in temperature, water content and pressure from values adopted as nominal. The adopted nominal stream conditions, to which the actual values in all the present experiments approximated, are a temperature of 22°C, standard atmospheric pressure, and a water content such that the wet-element temperature is 15°C.

With the aid of eqs (1) and (5) and the data of Appendix B, the contributions to the temperature difference from the known differences of the elements and of their local conditions can be calculated and the difference of their values of A_c derived. For the highest accuracy, the relative nominal sizes of the elements should have been chosen so that the elements are approximately "matched" in the sense that their radiation factors and hence their α factors are approximately equal. In particular, this greatly reduces the dependence of the comparison on the emissivity ϵ and evaporation coefficient α of the surface.

A practically exact general procedure for reducing element-comparison observations to the fractional difference of the values of A_c is given in Appendix A. An addition to the procedure, also given, yields the temperature difference

which the elements would have (with the derived difference in their values of A_c) if they were exactly of the nominal size (or sizes), widely separated, and exposed to an airstream of exactly the nominal conditions.

For a comparison of elements of the same type, only one $Nu(Re)$ function is involved and its uncertainty is of little consequence. However, with different types, two separately determined functions are involved and must be as accurate as possible, as for a 10 mm element at 1 m/s the effect of even a 1 percent error in the relative values is significant. Correspondingly, an error of 2 percent in the diameter (size) of an element is significant.

The enhancement of the velocity at an element due to a cylindrical second element has been found from velocity explorations with larger models to approximate that calculated for unseparated potential flow around the cylinder. Thus the local velocity of incidence v_i approximates

$$v_i = v \left[1 + \left(\frac{a}{w} \right)^2 \right], \quad (14)$$

where v is the free-stream velocity, a the radius and w the separation of the axes (Milne-Thomson [1968]). For flat-plate simulators (figure 1(b)), the effective radius has been taken to be one-half the mean thickness. For the nominal separation ($w = 6a$) a cylinder increases the velocity at the other element by approximately 2.8 percent.

Because part of the field of view from one element includes the other, a view factor required for h_r (see Appendix B) must be calculated for each which is that fraction of the radiation from the metal-cored section of the element which is not intercepted by the whole wet area of the other element. The two view factors have been calculated for each comparison by numerical evaluation of the appropriate fourfold integrals. For cylinders of the same diameter at the adopted separation the value is 0.947.

In the following, the results in figures 5 and 6 are plotted as temperature differences to give a proper impression of the magnitudes involved. Those in figure 5 have been reduced in accordance with Appendix A so that they relate to widely separated elements of exactly the nominal diameter and to the nominal airstream conditions. The results in figure 6 similarly relate to a wide separation and the nominal conditions but are for the actual diameters, as explained below. For figures 7, 8, 9, and 10, the results have been reduced to the fractional difference of the values of A_c of the elements. The elements are referred to by their nominal sizes throughout. The maximum departure of an actual size from the nominal has been several percent.

Each set of results given or referred to in the paper has been obtained in a single continuous sequence, and no observations have been discarded.

3.4. Reproducibility

To show the reproducibility for a given pair of elements and to illustrate some aspects of the comparison method, results are given in figure 5 for two 5 mm cotton-yarn covered elements at 5 m/s. Five series of measurements were made for angular positions from 0 to 360°. Each point plotted (center of a bar) represents the average for the particular angle over the five sets, while the half-length of the bar represents the standard deviation. The latter ranges from 1 mK or less for angles near 0 and 180°, to about 2 mK for angles on the flanks of the peaks at 90 and 270°. The curve drawn through the points is made up of a background completed in the figure by broken lines, and two superimposed peaks of 28 mK. The former represents the effect of the separated flow of each element on the flow around the other, and the latter represents that of the wake of each element impinging on the other.

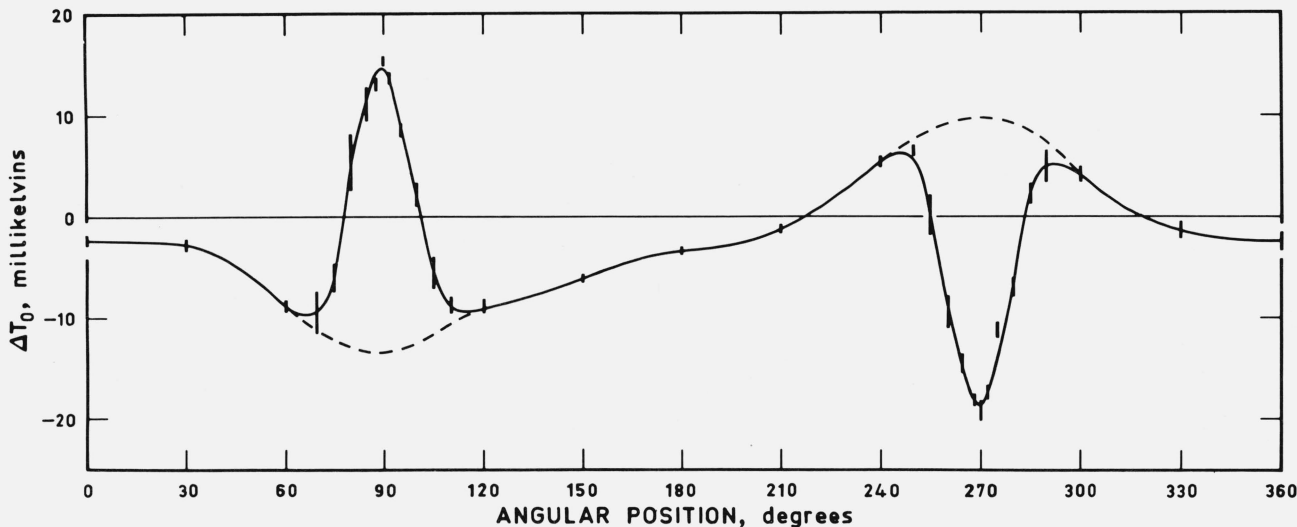


FIGURE 5. Temperature difference of two parallel 5 mm cotton-yarn covered wet elements 10 mm apart and perpendicular to an airstream of 5 m/s, for angular positions of 0 to 360° about their parallel axis of symmetry. Temperature depression 7 K. The standard deviation (half the error bar) is only 1 or 2 mK.

If we care to regard the two elements jointly as being a single element, we see that the relative smallness of the peaks (28 mK in 7 K) illustrates that different parts of a wet surface are practically at the same temperature even when the flow passes first over one part and then the other. The effects of the diminished temperature and the increased water content of the air incident on the downstream surface practically cancel. For laminar boundary-layer flow, this property has been predicted theoretically above. The 2.5 mK downwards displacement of the whole curve in figure 5 represents a real difference between the elements, possibly associated with minor irregularities of shape. (Errors in the

diameter measurements could contribute only about 0.7 mK.) All the results in the remainder of the paper represent measurements for angular positions of 0 and 180° averaged to cancel small effects arising from vertical gradients in the airstream.

The reproducibility from element to element has been studied both for cotton-yarn and grooved stainless-steel coverings. Four pairs of 5 mm cotton-yarn covered cylindrical elements compared at 5 m/s gave an average absolute temperature difference of 1.5 mK, the greatest difference being 2.5 mK. This high reproducibility, equivalent to approximately 0.1 percent in A , is surprising for elements so easily constructed. Two pairs of 5 mm stainless-steel covered elements compared at 2, 5, and 10 m/s, and another pair compared at 5 m/s, gave an absolute difference, averaged for the different pairs and different airspeeds, of only 0.4 mK, the greatest single difference being 1.4 mK. These differences are not significant. Further, no significant difference

could be detected between grooved stainless-steel coverings formed on a lathe and those formed on a thread-grinding machine.

3.5. Uniformity of the Surface Temperature

Heat-transfer calculations show that with the construction of figure 1(a) the high thermal conduction in the core may be expected to reduce substantially any nonuniformity of the surface temperature that would otherwise occur. The core itself is certainly isothermal. We may therefore test for any

significant effect of nonuniformity by deliberately increasing the thickness of the cotton covering.

Two nominally 10 mm cotton-yarn covered elements, actually differing in diameter by 0.7 percent, were compared at airspeeds of 1 to 10 m/s. The resulting temperature differences, adjusted to correspond to a wide separation and the nominal conditions but *not* adjusted for the departures of the diameters from the nominal, are shown in figure 6 along with the purely theoretical curve *A*. The curve departs from the horizontal line solely because of the diameter difference.

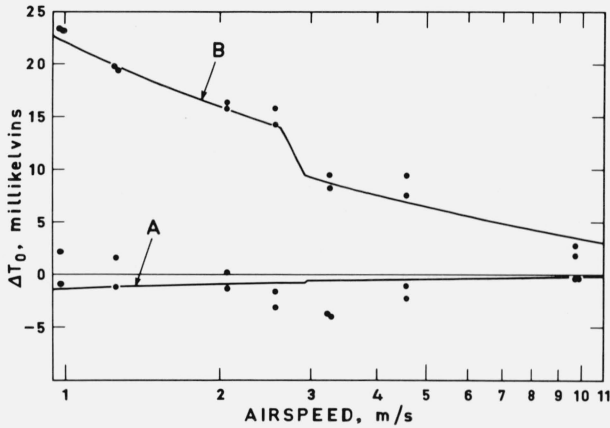


FIGURE 6. Effect on the temperature difference of two initially almost similar 10 mm cotton-yarn covered wet elements (purely theoretical curve *A* and associated experimental points) when the diameter of one is increased 12 percent by thickening its wet covering (purely theoretical curve *B* and associated experimental points.)

Temperature depression 7 K. The double kink is due to a kink in the $Nu(Re)$ plot for a cylinder, and for curve *B* is echoed by the experimental points.

The deviation of the points from the curve is 2 or 3 mK. The (slightly) smaller element was then increased 12.3 percent in diameter by the addition of a layer of white filter paper and a further winding of cotton yarn. The temperature differences then obtained, adjusted as before, are shown with the corresponding purely theoretical curve *B* in the same figure. There is no indication of any systematic departure of the points from the curve, and so it may be concluded that the effect of any nonuniformity of the temperature is negligible.

There are two other important aspects of these results. Firstly, they show agreement between the observed and calculated effects of a diameter difference. (At the same time, they illustrate that a diameter change of even 2 percent would be significant for a 10 mm element at the lower airspeeds.) Secondly, the double kink in the theoretical curves, which arises from the abrupt change in slope found experimentally in the heat-transfer relationship (given in Appendix B), is echoed in the experimental points. Thus a purely psychrometric experiment, which measures only a temperature effect, has provided independent confirmation of the kink in the heat-transfer relationship.

3.6. Effect of the Water-retaining Covering

Water-charged cylindrical stainless-steel surfaces have been seen above to behave precisely like smooth cylindrical water surfaces. The behavior of wet cotton-yarn covered surfaces has been determined by comparison with them. Results for 5 mm elements are given in figure 7, and results for 10 mm elements are given in figure 8. Three regions can be distinguished in the curves drawn through the experimental points. In the low-air-speed region, small departures from the central plateaus occur which probably represent no more than the systematic errors of 1 to 2 percent which inevitably exist in the specially measured heat-transfer relationships.

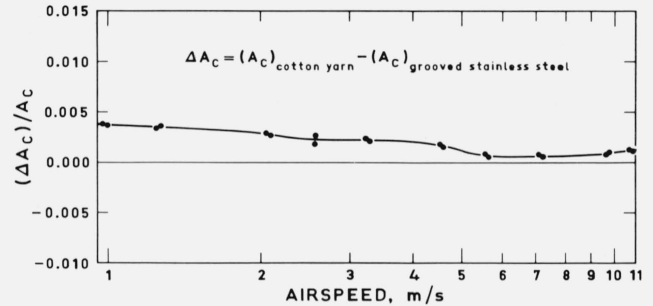


FIGURE 7. Fractional difference of the convective psychrometer coefficients A_c for a 5 mm cotton-yarn covered wet element and a 5 mm wet element with grooved stainless-steel covering.

These experimental results and those of Figure 8 relate the A_c for a cotton-yarn covered cylinder to that for a smooth cylinder of water.

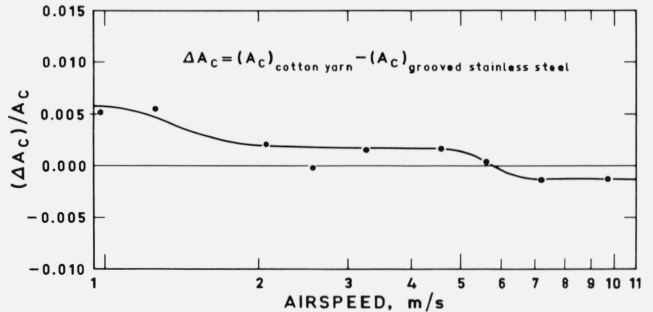


FIGURE 8. Fractional difference of the convective psychrometer coefficients A_c for a 10 mm cotton-yarn covered wet element and a 10 mm wet element with grooved stainless-steel covering.

(See also the legend of Fig. 7.)

At the higher airspeeds, departures occur which are believed to be associated with observed wavelike disturbances of the water surface, the effect for the grooved surface predominating. Indeed, at 10 m/s the local pressure varies around the circumference by about 25 mm head of water. The effect sets in at about the same airspeed for both diameters rather than at the same Reynolds number. The discordant point at approximately 2.6 m/s in figure 8 corresponds with the kink

in the $Nu(Re)$ relationship for the cotton-yarn covered cylinder. If in the reduction of the results this kink is regarded as rounded by about 2 percent, the point is brought on to the curve.

The plateau regions in the figures may be considered substantially free of these effects, and give the difference in A_c as 0.22 and 0.17 percent, respectively. Figure 7 establishes that the effect of the cotton-yarn covering is to increase A_c by approximately 0.2 percent for Reynolds numbers from about 800 to 1400, while figure 8 establishes the same result for Reynolds numbers from 1400 to 3000. It would be surprising if the result did not extend to Reynolds numbers well below 800, the airspeed being kept below about 5 m/s.

No significant change in A_c or its trend occurs for either type of element when the airspeed passes through the value for the kink in the corresponding $Nu(Re)$ relationship; for in figure 7 the kink corresponds to 3.0 m/s for the grooved element and in figure 8 to 2.6 m/s for the cotton-yarn covered element; and both airspeeds lie well within the respective plateaus. Thus the $Nu(Re)$ and $Sh(Re)$ relationships must be similarly kinked, as the similarity principle would suggest, and the dependence of Nu on Pr (and equally of Sh on Sc) must be much the same above and below the kink. Further, as the related heat-transfer measurements have shown that $Nu(Re)$ is affected by the free-stream turbulence above but not below the kink, we may conclude that the results of figures 7 and 8 have not been affected by the turbulence except possibly in the region of the downturn at high airspeeds.

3.7. Absolute Values of A_c

Because of the similarity of eqs (7) and (8) and the near equality of Pr and Sc for water in air, wet elements which have approximately the same heat-transfer coefficients must have values of A_c that are still much more closely the same. For a range of the Reynolds number the measured heat-transfer coefficients given in Appendix B for the simulators not only have accurately the flat-plate Reynolds-number dependence but are only about 3 percent greater than the flat-plate value in magnitude. Consequently, with allowance for the effect of the cotton-yarn covering, found above to be 0.2 percent, A_c for the simulator may be estimated to approximate the flat-plate value to much better than 1 percent. In another view, we note that regarding convective transfer properties, the simulator is much closer to the flat plate than to the cylinder. However, it will shortly be seen that A_c for the cylinder is only 0.7 percent greater than for the simulator; and so again we conclude that, with allowance for the effect of the covering, A_c for the simulator must approximate the flat-plate value to much better than 1 percent. Therefore, although the simulator must shed its boundary layers near its blunt trailing edge, its value of A_c is

practically that given by the theory with the flat-plate function ϕ .

The absolute value of A_c for the cylinder may be found by comparison with the simulator, the relative sizes of the elements being chosen for approximate matching as defined in section 3.3. Observations are made for angular positions of 0 and 180° and averaged, but when the two-element unit is turned between these positions the simulator must also be turned 180° about its own axis.

Figure 9 gives results for a 5 mm grooved cylinder and a simulator (cotton-yarn covered), the semiperimeter of whose overall cross section is 9 mm, and figure 10 gives results for a 10 mm cotton-yarn covered cylinder and a simulator of 18 mm semiperimeter. In each case three regions analogous to those identified in figures 7 and 8 can be distinguished in the curves drawn through the experimental points. The downturn at the higher airspeeds corresponds approximately with the commencement of an observed rise of the simulator heat-transfer coefficient above flat-plate values.

From the plateau region in figure 9 we see that for at least the Reynolds number range 650 to 1600, the value of A_c for

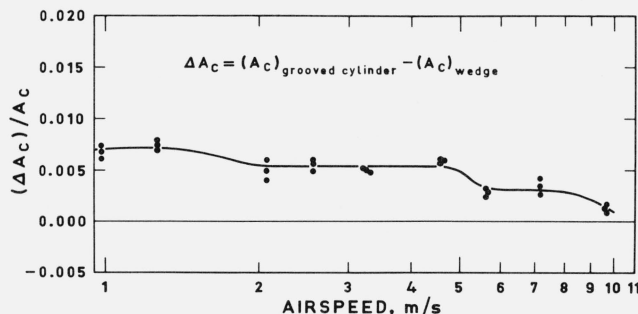


FIGURE 9. Fractional difference of the convective psychrometer coefficients A_c for a 5 mm wet-element with grooved stainless-steel covering and a cotton-yarn covered flat-plate simulator 9 mm wide (Fig. 1 (b)).

These experimental results and those of Figure 10 relate the A_c -values of the cylindrical wet elements to the theoretical value for the classical flat plate system.

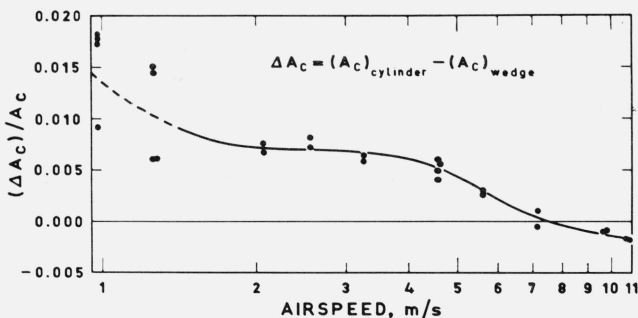


FIGURE 10. Fractional difference of the convective psychrometer coefficients A_c for a 10 mm cotton-yarn covered wet element and a cotton-yarn covered flat-plate simulator 18 mm wide (Fig. 1 (b)).

(See also the legend of Fig. 9.)

the grooved cylinder exceeds that for the cotton-yarn covered simulator by approximately 0.54 percent. As the results for the effect of the cotton-yarn covering averaged 0.20 percent, the corresponding excess for similar coverings is 0.74 percent. From figure 10, which involves no difference in the coverings, we find that for at least the Reynolds number range 1200 to 2500, the excess is 0.70 percent.

Adopting a rounded value of 0.7 percent and referring to the value of A_c given in section 2.4 for the flat plate, we conclude that for atmospheric pressure and wet-element temperatures in the general neighborhood of 15 °C, and for at least the Reynolds number range 650 to 2500, the value of A_c for a smooth cylinder of water is $5.83 \times 10^{-4} K^{-1}$ while that for a cotton-yarn covered cylinder is $5.84 \times 10^{-4} K^{-1}$. Again, it would be surprising if these results did not extend to much lower Reynolds numbers, the airspeed being kept below about 5 m/s. More generally, for a cotton-yarn covered cylinder A is given by eqs (5) and (11) with B_c 0.9 percent greater than given by eq (13).

3.8. Uncertainties in the Results

The uncertainty introduced by calculating the fractional difference of A_c from element-comparison observations (see appendix A) is associated with the quantities h_r/h_c and k_c/k_α in eq (5), and for comparisons of elements approximately matched in the sense of section 3.3 arises in general from the measurements of the sizes of the elements, the estimates of their local airspeeds of incidence, and the uncertainties in the $Nu(Re)$ functions used. It is convenient to regard the uncertainty in each $Nu(Re)$ function as concentrated in the coefficient b of eq (7). As k_c in eq (5) is proportional to h_c , and Nu is approximately proportional to $Re^{1/2}$, h_r/h_c is approximately proportional to and k_c/k_α inversely proportional to $(d/v_i)^{1/2}/b$, where d is the element diameter or, for the flat-plate simulator, semiperimeter and v_i is the local airspeed of incidence as in eq (14). Thus the effect of the errors in d , v_i and b on each radiation factor is partly offset by their effect on the associated α factor.

Measurements of the diameters of the same cotton-yarn covered cylindrical elements over a period have shown that the uncertainty in the diameter is 0.8 percent for $d = 5$ mm and 0.4 percent for $d = 10$ mm. (All the given uncertainties represent three times the standard deviation.) The corresponding uncertainty for a grooved stainless-steel covering is negligible. The uncertainty in the semiperimeter of a simulator is approximately the same as in the diameter of a matching cotton-yarn covered cylinder—0.8 percent for a semiperimeter of 9 mm and 0.4 percent for 18 mm. The uncertainty in the relative local airspeeds is significant only for comparisons of cylinders with flat-plate simulators, for which it is estimated to be 1 percent. That in the relative values of b is significant only for dissimilar elements, and for such is 2 percent.

Summing the squares of the independent component uncertainties, the uncertainty in deriving the fractional difference in A_c for the middle of the plateau is found to be 0.13 percent (of A_c) for figure 7, 0.16 percent for figure 8, 0.13 percent for figure 9, and 0.17 percent for figure 10. As the comparison experiments give the fractional difference of the values of A within 0.05 percent (of A), the overall uncertainties in the fractional differences of A_c are only slightly greater than these values. Clearly, the uncertainty in the absolute value of A_c derived for a cotton-yarn covered cylinder is practically only the uncertainty of 1 percent in the theoretical A_c for a smooth-wave flat plate or simulator.

When eq (5) is used to obtain A from A_c in a particular case, a further uncertainty is introduced which depends not only on those in d , v_i and the $Nu(Re)$ function, but also those in h_r and k_α , which are attributable, respectively, to the emissivity ϵ and the evaporation coefficient α . The uncertainty in ϵ and hence h_r is 1.5 percent. As the value of α has been obtained from element-comparison experiments (see Appendix B), the uncertainty to be assigned to it here is less than the absolute uncertainty, and it has been taken to be 30 percent. Then, for example, for a cotton-yarn covered cylinder 3 ± 0.15 mm in diameter and an airspeed of incidence of 3 ± 0.15 m/s the further uncertainty is 0.4 percent and the calculated overall uncertainty 1.1 percent—still little more than 1 percent.

Direct measurements of the psychrometer coefficient for cotton-yarn covered cylinders in a transverse stream have been made by Wylie and Lalas (to be published) and give A_c with an absolute uncertainty of only 0.3 percent. The measurements are for Reynolds numbers of 60 to 600 and various wet-element temperatures. This Reynolds number range does not overlap the present range but, on the basis that A_c does not depend significantly on the Reynolds number, the direct results are consistent with the error in the present results being considerably less than 1 percent.

4. Conclusions and Applications

4.1. Conclusions

Except for the larger elements at the lower airspeeds, the technique of comparing wet elements by direct measurement of their temperature difference in a common airstream allows the difference of their psychrometer coefficients A to be determined within 0.05 percent (of A). With the use of heat-transfer data obtained experimentally for elements of the types used, the overall uncertainty in the derived difference of the convective psychrometer coefficients A_c is less than 0.07 percent for nominally similar elements and less than 0.2 percent for elements which differ in type but are approximately matched as regards their radiation and α factors.

Easily constructed cotton-yarn covered cylindrical elements have been described which have a common value of A_c within 0.1 percent. Their wet surfaces do not depart significantly from temperature uniformity. The elements with grooved stainless-steel surfaces are still more reproducible from element to element; but are to be regarded as a research tool, not being sufficiently easy to manage for general use. By comparisons with these elements and with bladelike elements which, as regards their heat-transfer and hence psychrometric properties, closely simulate the classical flat-plate system, the relationship between the psychrometer coefficient for a cotton-yarn covered cylinder and that for the latter system has been established with an uncertainty of about 0.2 percent. The absolute value of A_c for such an element has thereby been determined within approximately 1 percent while, in work yet to be published, A_c has been measured directly for that type of element with an absolute uncertainty of only 0.3 percent.

Ferrel's [1885] value of A for a cylinder 4 to 5 mm in diameter in a transverse stream of 5 to 7.5 m/s is easily shown to be about 8 percent too high. With a suitably calculated value of h_c , Sprung's [1888] value for a rounded cylinder 10 mm long in an axial stream of approximately 2.3 m/s with the radiative heat transfer reduced to about one-third by a shield can be shown to be about equally too high. The bias may have resulted from effects due to organic films and the practical limitations of reference dew-point hygrometers.

4.2. Water Vapor Measurements

A simple specification for a psychrometer can be produced which ensures that instruments made to and operated in accordance with the specification by different laboratories have accurately the same psychrometer coefficient. For example, if the specification called for a 3 mm cotton-yarn covered cylinder in a transverse airstream of 3 m/s, with a tolerance of 5 percent on both the diameter and the airspeed, the different instruments would have values of A within 0.16 percent of a universal value. A capillary water feed could be used. If the laboratories measured temperature accurately, their measurements of, for example, a vapor partial pressure of 1000 Pa (10 millibars) at 20 °C and atmospheric pressure would be within 0.07 percent of a common value. In fact the appropriate universal value of A is known within 0.3 percent; and the absolute accuracy of the vapor pressure measurements would be 0.12 percent, corresponding to the difference between 42.61 and 42.66 percent relative humidity.

A practical reference psychrometer based on the work has been developed by Wylie and Lalas for the World Meteorological Organization. This was adopted by the WMO Commission for Instruments and Methods of Observation [1977] as the reference standard for meteorological humidity mea-

surements at the earth's surface such that the wet-element temperature is not below 0 °C. An account of it is to be published by WMO in 1979.

The high stability of well-designed wet elements makes them very suitable for differential instruments. For example, an entrained gas stream may be divided into two branches, one flowing through a small chamber containing a research subject, such as the unsevered leaf of a plant, and the other serving as a reference. Nominally similar elements with continuous capillary water feeds may be installed in the emerging streams in a region where they have been accurately equalized in temperature by passage through a simple parallel flow heat exchanger. A zero stability of better than 0.05 percent in A can be obtained. (The zero can be checked by allowing the working stream to bypass the experimental chamber.) Considering again a vapor pressure of 1000 Pa at 20 °C and atmospheric pressure, this corresponds to less than 0.02 percent in the vapor pressure. An important property of the wet elements, very advantageous for this application, is their complete freedom from hysteresis effect.

Before the need for the precautions explained in sections 1.2 and 3. was properly understood, the author developed differential psychrometers for use in plant and animal physiology. Modified forms of these have been used in experiments with plants by Slatyer and Bierhuizen [1964] and experiments with animals by Allen and Bligh [1969]. A substantial improvement in the instrumentation would now be possible.

4.3. Evaporation Coefficient of Water

When wet elements of substantially different diameters are compared, as in the experiment of figure 6 (curve B), a temperature difference is observed which at low airspeeds originates mainly from the radiative heat transfer and is proportional to the emissivity ϵ , but at high airspeeds contains a considerable component which originates from the α -effect and is proportional to α^{-1} . The effect of α can be increased by using the smallest practicable diameter in conjunction with a much larger diameter. Values of ϵ and α can then be derived with the aid of eqs (1) and (5).

Results have been obtained by Wylie and Lalas (to be published) using diameter ratios as large as four. Unlike former methods of measuring α , which have been controversial, the method involves only slow evaporation from quiescent water surfaces. The value found for ϵ agrees with that deduced from infrared reflectance measurements. This value and a rounded value of α are given in Appendix B.

4.4. Evaporation Resistance of a Monomolecular Film

The presence of a monomolecular film on a wet element can add greatly to the evaporation resistance provided by the α -effect. The possibility of using present methods to measure

even small film resistances for purposes of fundamental studies is apparent from table 1 and the text of section 4.3. From the results of table 1, we can deduce that the additional evaporation resistance (i.e., addition to the reciprocal of k_α) when the oleic acid monolayer is present is 3×10^{-3} (mole-fraction difference)/(mol·s⁻¹·m⁻²). Work on this application is continuing.

4.5. Convective Heat-transfer Measurements

A method for wet surfaces which depends on the present work has been described by Wylie and Lalas [1973] during its development. Since fully developed, it gives a standard deviation of better than 2 percent for the individual measurements and an absolute accuracy of 1 to 2 percent. As in some methods used for liquid drops, reviewed by Fuchs [1959], and the elaborate experiments of Dahlen [1962], the psychrometric behavior of the wet surface maintains a depressed and practically uniform surface temperature. The heat influx is determined from the loss in weight due to evaporation and, after corrections, gives the heat-transfer coefficient (not the mass-transfer coefficient). Heat-transfer formulas obtained by this method for the present types of elements are given in appendix B. A full account of the measurements will be published.

5. Appendix A. Reduction of Element-comparison Results

Measured are the stream temperature T , pressure p , velocity v and reference wet-element temperature $T_{O,R}$, the diameters (generally, characteristic lengths) d_R , d_1 , and d_2 of the elements, other geometrical details relating to the elements which lead to the local velocities of incidence v_R , v_1 and v_2 and to the view factors F_1 and F_2 (F_R is unity), and the difference of the wet-element temperatures $\Delta T_O = T_{O,2} - T_{O,1}$. The heat-transfer coefficients h_c and h_r , the mass-transfer coefficients k_c and k_α , and hence the radiation and α factors of eq (5), are calculated using the Nusselt numbers, formulas and data of Appendix B, the fluid properties being evaluated for the temperature and composition of the gas at each wet-element surface as explained in section 2.3 of the text.

The following procedure yields the fractional difference of the values of A_c of the elements. The coefficient $A_{c,1}$ and $A_{c,R}$ are simply assigned the best values available. The optional second stage yields the corresponding temperature difference $(\Delta T_O)_N$ for the nominal conditions T_N , p_N , v_N and $(T_{O,1})_N$ of the stream, and for nominal characteristic lengths $d_{1,N}$ and $d_{2,N}$ and a wide separation of the elements ($v_2 = v_1 = v_N$ and $F_{2,N} = F_{1,N} = 1$). In steps 3 and 11, it may be sufficient to employ eqs (5) and (1) consecutively rather than simultaneously.

Step	Values used	Equation(s)	Result
STAGE 1			
1	$T, T_{O,R}, p, d_R, v_R$, with Nu_R	Eq (5)	A_R
2	$T, T_{O,R}, p, A_R$	Eq (1)	x
3	T, p, x, d_1, v_1, F_1 , with Nu_1	Eqs (1) and (5) simultaneously	$T_{O,1}$
4	$T_{O,1}, \Delta T_O$	$T_{O,2} = T_{O,1} + \Delta T_O$	$T_{O,2}$
5	$T, T_{O,2}, p, d_2, v_2, F_2$, with Nu_2	Eq (5)	$(A_2/A_{c,2}) = \eta$
6	$T, T_{O,2}, p, x$	Eq (1)	A_2
7	η, A_2	$A_{c,2} = A_2/\eta$	$A_{c,2}$
8	$A_{c,1}, A_{c,2}$	$\frac{\Delta A_c}{A_{c,1}} = \frac{A_{c,2} - A_{c,1}}{A_{c,1}}$	$(\Delta A_c)/A_{c,1}$
STAGE 2			
9	$T_N, (T_{O,1})_N, p_N, d_{1,N}, v_N, F_{1,N} = 1$, with Nu_1	Eq (5)	$A_{1,N}$
10	$T_N, (T_{O,1})_N, p_N, A_{1,N}$	Eq (1)	x_N
11	$T_N, p_N, x_N, d_{2,N}, v_N, F_{2,N} = 1$, with Nu_2	Eqs (1) and (5) simultaneously	$(T_{O,2})_N$
12	$(T_{O,1})_N, (T_{O,2})_N$	$(\Delta T_O)_N = (T_{O,2})_N - (T_{O,1})_N$	$(\Delta T_O)_N$

6. Appendix B. Dimensionless Groups, Transfer Coefficients and Property Values

6.1. Dimensionless Groups

The Nusselt number Nu , Sherwood number Sh , Prandtl number Pr , Schmidt number Sc and Reynolds number Re are defined by

$$Nu = h_c d / \lambda, \quad Sh = k_c d / (cD),$$

$$Pr = \mu c_p / \lambda, \quad Sc = \mu / (\rho D),$$

$$\text{and } Re = \rho d v / \mu,$$

where h_c is the convective heat-transfer coefficient, k_c the convective vapor-transfer coefficient with the same units as

a mole flux density, d the characteristic length (diameter or, for a flat-plate simulator, the semiperimeter), v the local stream velocity, c , ρ , c_p , μ and λ are, respectively, the total mole density, mass density, specific heat, dynamic viscosity and thermal conductivity of the gas, and D is the diffusivity of the vapor.

6.2. Heat- and Mass-transfer Coefficients

From measurements made in the wind tunnel under the conditions of the present work, $\log_{10}Nu$ for the surface-average convective heat-transfer coefficients for the wet elements has been found to be a linear or quadratic function of $\log_{10}Re$, with coefficients as follows. The absolute accuracy is 1 to 2 percent.

System	Range of Re	B_0	B_1	B_2
cotton-yarn wound cylinders	100-1850	-0.1922	0.4607	-
	1850-11000	-0.6784	0.6095	-
5 mm grooved cylinder	300-1000	-0.1965	0.4607	-
	1000-3500	0.9863	-0.3969	0.15428
10 m grooved cylinder	600-1200	-0.1965	0.4607	-
	1200-7000	0.5407	-0.1022	0.10518
9 mm flat-plate simulator*	550-2100	-0.2167	0.5	-
	2100-2800	-0.4181	0.5606	-
	2800-7000	-0.2733	0.5186	-
18 mm flat-plate simulator†	1100-3700	-0.2159	0.5	-
	3700-12000	-0.6968	0.6348	-
	12000-14000	-0.1469	0.5	-

* Short connecting line; precise form uncertain.
 † Short third branch; precise form uncertain.

The lower branches for the grooved cylinders are approximately 2 percent (in Nu) below the lower branch for cotton-yarn covered cylinders, but about 3 percent above the corresponding branch of the relationship recommended by Morgan [1975] for smooth dry cylinders. The lower branches for the flat-plate simulators are uniformly approximately 3 percent above the theoretical result for the true flat plate. All the lower branches have been practically unaffected by the 1 percent of free-stream turbulence in the wind tunnel.

The Prandtl boundary-layer equations (see Schlichting [1968]) may be solved numerically for the classical flat-plate system with negligible mass transfer and uniform fluid properties to give

$$Nu = 0.664115 Re^{1/2} \phi(Pr),$$

where $\phi = 1$ when $Pr = 1$, and where for $0.4 < Pr < \infty$, and to within 1 in 10^5 ,

$$\phi(Pr) = (C_0 + C_1/Pr + C_2/Pr^2 + C_3/Pr^3 + C_4/Pr^4) Pr^{1/3},$$

the coefficients being

$$\begin{aligned} C_0 &= 1.0200524, & C_1 &= -2.26598 \times 10^{-2}, \\ C_2 &= 3.0170 \times 10^{-3}, & C_3 &= -4.4897 \times 10^{-4}, \\ C_4 &= 3.9020 \times 10^{-5}, & & \end{aligned}$$

The sum of the coefficients is naturally unity.

For the α factor in eq (5) we may obtain k_c from eq (6) with $A_c = 5.8 \times 10^{-4} \text{ K}^{-1}$.

From the Stefan-Boltzmann equation, we find that h_r is given with ample accuracy by

$$h_r = 4.622 F \epsilon \left(\frac{T_m}{273.15} \right)^3 \text{ watt} \cdot \text{m}^{-2} \cdot \text{K}^{-1},$$

where T_m is the arithmetic mean of T and T_0 , F is the view factor defined in section 3.3, and ϵ is the emissivity inferred from infrared reflectance measurements with representative wet surfaces to be 0.98.

The mass-transfer coefficient k_α of the α -resistance is found by the method of Monchick and Reiss [1954] to be given by

$$k_\alpha = \frac{2cW\alpha}{(2-\alpha)},$$

where c is the total mole density of the gas, α the evaporation coefficient, and

$$W = [RT_0/(2\pi M)]^{1/2},$$

R being the gas constant and M the molecular weight of the vapor. The value of α from measurements made as in section 4.3, rounded to 0.06, has been used.

6.3 Property Values

The second virial coefficient of dry air has been taken from Sengers et al. [1971] and that of water vapor from Goff [1949]; while the binary interaction coefficient for the mixture has been taken from Hyland and Wexler [1973] and Wylie and Fisher [1974], and differs significantly from that of Goff. The density of the mixture has been calculated using these coefficients.

The vapor pressure of pure water has been taken from Wexler [1976]. The factor f_w introduced in section 2.2 has been calculated with the aid of the virial and interaction coefficients, and the heat of evaporation with the aid of those coefficients and the heat of evaporation of pure water given by Osborne, Stimson, and Ginnings [1939]. For standard atmospheric pressure and temperatures of 0 to 70° C, the ratio r of the heat of evaporation to that of pure water is found to be given to within 1 in 10^4 by

$$r = 1 - (6.3 \times 10^{-4} + 8.6 \times 10^{-6} T + 1.61 \times 10^{-7} T^2),$$

with T in $^{\circ}\text{C}$. The specific heat of the mixture has been calculated from the virial and interaction coefficients and the zero-pressure thermodynamic data of Hilsenrath et al. [1960].

The viscosity and thermal conductivity of moist air have been taken from Mason and Monchick [1965], but the latter quantity has been adjusted progressively to the Thermophysical Properties Research Center [1970] values for zero-water content. The vapor diffusivity has been assessed from a number of references to be $2.58 \times 10^{-5} \text{ m}^2 \text{ s}^{-1}$ at 25°C and proportional to the 1.8 power of the absolute temperature. For the present T_0 this gives a value 0.8 percent greater than Kusuda's [1965].

The author is most appreciative for the extensive assistance of Mr. Theo Lalas in the conduct of the experiments.

7. References

- [1] Allen, T. E., and Bligh, J. (1969), *Comp. Biochem. Physiol.* **31**, 347.
- [2] Assmann, R. (1887), *Das Wetter* **4**, 265.
- [3] August, E. F. (1825), *Ann. Physik* **5**, 69.
- [4] Bedingfield, C. H., Jr., and Drew, T. B. (1950), *Ind. Eng. Chem.* **42**, 1164.
- [5] Belli, G. (1830), *Corso elementare di fisica sperimentale*, vol. 2, p. 499 (Liceo, Milan).
- [6] Bird, R. B., Curtiss, C. F., and Hirschfelder, J. O. (1955), *Chem. Eng. Progr. Symp. Ser.* **51**, 69.
- [7] Bird, R. B., Stewart, W. E., and Lightfoot, E. N. (1960), *Transport phenomena* (Wiley and Sons, New York).
- [8] Böckmann, C. W. (1803), *Ann. Physik (Gilbert)* **15**, 355.
- [9] Bongards, H. (1926), *Feuchtigkeitsmessung* (Oldenbourg, Munich).
- [10] Colburn, A. P. (1932), *Am. Inst. Chem. Engrs.* **28**, 105.
- [11] Dahlen, R. J. (1962), A relation between heat and mass transfer coefficients verified for adiabatic evaporation from a cylinder. Ph.D thesis, Purdue University.
- [12] Eckert, E. R. G., and Drake, R. M., Jr., (1959), *Heat and mass transfer*, 2nd ed. (McGraw-Hill, New York).
- [13] Ferrel, W. (1885), Annual report of the Chief Signal Officer of the Army to the Secretary of War for the year 1886, Appendix 24 (Washington, D.C.).
- [14] Fuchs, N. A. (1959), Evaporation and droplet growth in gaseous media, trans. by J. M. Pratt (Pergamon, London).
- [15] Goff, J. A. (1949), *Trans. ASME* **71**, 903.
- [16] Hilsenrath, J., et al., (1960), *Tables of thermodynamic and transport properties* (Pergamon, Oxford).
- [17] Hutton, J. (1792), See Playfair (1805), *Edinburgh Trans. Roy. Soc.* **5**, part III, 39.
- [18] Hyland, R. W., and Wexler, A. (1973), *J. Res. Nat. Bur. Stand. (U.S.)* **77A**, 133.
- [19] Jarvis, N. L., Timmons, C. O., and Zisman, W. A. (1962), Retardation of evaporation by monolayers: Transport processes, ed. by V.K. La Mer, pp. 41-58 (Academic Press).
- [20] Kusuda, T. (1965), *Humidity and moisture*, ed. by A. Wexler, vol. 1, pp. 16-32 (Reinhold, New York).
- [21] Leslie, J. (1799), *Nicholson's J. Nat. Phil.* **3**, 461 and 518.
- [22] Makarevicius, V., and Zukauskas, A. (1972), See Zukauskas [1972], p. 113.
- [23] Mason, E. A., and Monchick, L. (1965), *Humidity and moisture*, ed. by A. Wexler, vol. 3, pp. 257-272 (Reinhold, New York).
- [24] Milne-Thomson, L. M. (1968), *Theoretical hydrodynamics*, 5th ed., p. 158 (Macmillan, London).
- [25] Monchick, L., and Reiss, H. (1954), *J. Chem. Phys.* **22**, 831.
- [26] Morgan, V. T. (1975), *Advan. heat transfer*, vol. 11, p. 199 (Academic Press).
- [27] Osborne, N. S., Stimson, H. F., and Ginnings, D. C. (1939), *J. Res. Nat. Bur. Stand. (U.S.)* **23**, 197.
- [28] Schlichting, H. (1968), *Boundary-layer theory*, trans. by J. Kestin, 6th ed. (McGraw-Hill, New York).
- [29] Sengers, J. M. H. L., Klein, M., and Gallagher, J. S. (1972), *Am. Inst. Phys. Handbook*, 3rd ed., section 4i, p.212 (McGraw-Hill, New York).
- [30] Sherwood, T. K. (1937), *Absorption and extraction*, 1st ed., chapter II (McGraw-Hill, New York).
- [31] Sinha, E. (1962), *Meteorological and Geostrophical Abstr.* **13**, 3622.
- [32] Slatyer, R. O., and Bierhuizen, J. F. (1964), *Plant Physiol.* **39**, 1051.
- [33] Sonntag, D. (1967), *Hygrometrie*, part 2 (Akademie-Verlag, Berlin).
- [34] Sprung, A. (1888), *Das Wetter* **5**, 105.
- [35] Squire, H. B. (1938), *Modern developments in fluid dynamics*, ed. by S. Goldstein, vol. II, p.631 (Clarendon Press, Oxford).
- [36] Stewart, W. E. (1963), *Am. Inst. Chem. Engrs.* **9**, 528.
- [37] Threlkeld, J. L. (1962), *Thermal environmental engineering*, 1st ed., chapter 10 (Prentice-Hall, N.J.).
- [38] TPRC (1970), *Thermophysical properties of matter*, vol. 3, Thermophysical Properties Research Center, Purdue University (IFI/Plenum, New York).
- [39] Wexler, A. (1976), *J. Res. Nat. Bur. Stand. (U.S.)* **80A**, 775.
- [40] WMO, Commission for Instruments and Methods of Observation (1977), Abridged final report of the seventh session, Hamburg, August 1977, WMO-No. 490 (WMO, Geneva).
- [41] Wylie, R. G. (1949), *Psychrometry*, National Standards Laboratory Report PA-4 (CSIRO, Sydney).
- [42] Wylie, R. G. (1973), *Chem. Eng. J.* **6**, 1.
- [43] Wylie, R. G., and Fisher, R.S. (1974), Accurate determination of the molecular interaction in a gas-vapour mixture, Fifth National Convention of the Royal Australian Chemical Institute, Canberra, May 1974, Physical Chemistry (RACI, Melbourne).
- [44] Wylie, R. G., and Lalas, T. (1973), The measurement of heat-transfer coefficients using psychrometric wet elements, First Australasian Conference on Heat and Mass Transfer, Melbourne, May 1973 (Monash University, Melbourne).
- [45] Zukauskas, A. (1972), *Advances in heat transfer*, vol. 8, p. 93 (Academic Press).